

Exploiting Tensor Structure for Computing Bound States of the Quantum Mechanical Three-Body Problem

Jonas Thies^a, Moritz Travis Hof^b, Matthias Zimmermann^c, Maxim Efremov^c

^a*Delft Institute of Applied Mathematics, Faculty of Electrical Engineering, Mathematics and Computer Science, Delft University of Technology Delft, The Netherlands*

^b*Department of High Performance Computing, Institute for Software Technology, German Aerospace Center (DLR), Cologne, Germany*

^c*Department of Theoretical Quantum Physics, Institute of Quantum Technologies, German Aerospace Center (DLR), Ulm, Germany*

Abstract

We develop a computationally and numerically efficient approach to determine binding energies and corresponding wave functions of a quantum-mechanical three-body problem in low dimensions. Our approach exploits the tensor structure intrinsic to the multidimensional stationary Schrödinger equation, which we express as a discretized eigenvalue problem. In order to obtain numerical solutions of the three-body system in one spatial dimension, we represent the Hamiltonian operator as a series of dense matrix-matrix products and propose an efficient preconditioned Jacobi-Davidson QR iteration for the resulting algebraic eigenvalue problem. This implementation allows a significantly faster computation of three-body bound states with a higher accuracy than in previous works. To investigate the feasibility of solving higher dimensional problems, we also consider the two-dimensional case where we make use of an efficient shared-memory parallel implementation. Our novel approach is of high relevance for investigating the universal behavior of few-body problems governed only by the particle masses, overall symmetries, and the dimensionality of space. Moreover, our results have straightforward applications in the physics of ultracold atomic gases that are nowadays widely utilized as quantum sensors.

Keywords: Schrödinger equation, three-body problem, pseudospectral method, tensor product structure, Jacobi-Davidson method

1. Introduction

The quantum-mechanical few-body problem is of particular interest for the physics community. On the one hand, it determines the features of interacting nuclei, atoms, or molecules as bodies living on very different length scales. On the other hand, in certain regimes these systems display a universal behavior that is

independent of the details of the interaction between the particles, but governed by the particle masses, overall symmetries, as well as the dimensionality of space. The complexity and beauty of this problem has motivated numerous researchers to explore these systems using theoretical, numerical, and experimental approaches.

An outstanding example for the above mentioned type of universality is the Efimov effect [1, 2], describing the emergence of an infinite sequence of universal states of three bosonic particles with s -wave resonant pair interactions in three dimensions. Moreover, lower dimensional systems, such as three fermionic particles confined to two dimensions, display surprising universal phenomena like the so-called ‘super Efimov effect’ [3, 4, 5, 6]. Recently, some of the authors have demonstrated that in one dimension, universality in a mass-imbalanced three-body system is not only present in the discrete spectrum [7], but universal three-body bound states also occur in the continuum as induced by excited two-body resonances [8].

In order to provide an adequate model of these systems, novel analytical and numerical tools are required. With an increasing number of particles or dimensions, accurate predictions of the properties of the quantum system become very challenging. For instance, in Ref. [7] three-body energies and the corresponding wave functions of the bound states are computed by representing the Hamiltonian as a sparse matrix, and using a Krylov subspace method to determine its lowest eigenvalues and the corresponding eigenvectors. However, with an increasing number of grid points in each dimension, the matrices and vectors grow rapidly: The three-body problem in d space dimensions yields a $2d$ -dimensional linear eigenvalue problem after removing the center-of-mass degree of freedom. When discretized with n grid points in each direction, a single vector that represents the three-body wave function has the size n^{2d} . Moreover, the pseudo-spectral discretization used in [7] leads to $\mathcal{O}(n^{2d-1})$ dense blocks in the sparse matrix representation of the Hamiltonian, each of size $n \times n$. Thus, such an approach is severely limited by the ‘curse of dimensionality’.

In this article, we present a novel numerical approach to analyze the three-body problem. In particular, we exploit the tensor product structure of the problem to avoid storing redundant blocks in the matrix. In this way we achieve very high computational efficiency. Moreover, in order to accelerate the convergence compared to the previously used Krylov method, we use the Jacobi-Davidson iteration scheme and introduce a preconditioner for the one dimensional (1D) three-body system. We then show how the approach can be extended to 2D, as a first step towards simulating quantum systems in 2D and 3D, or with a larger number of particles involved.

Our article is structured as follows. In Section 2 we introduce quantum-mechanical few-body systems in low dimensions and present the corresponding

eigenvalue equations determining the energies and stationary wave functions. In Section 3 we describe the discretization scheme and how it naturally enables a tensor formulation of the Hamiltonian operator. The Jacobi-Davidson iteration scheme is revisited in Section 4, and the implementation of the discretized operators in 1D and 2D are discussed in terms of hardware efficiency. For the 1D case, we devise a novel preconditioning technique to accelerate the convergence of the Jacobi-Davidson method. We apply it to determine the few lowest eigenpairs by solving the corresponding eigenvalue problem. Numerical results are then presented in Section 5. They show the superior performance and convergence properties of our method. Finally, in Section 6 we provide concluding remarks and indicate directions of future research.

2. Few-body systems

First, we consider a system composed of two interacting particles, a heavy one of mass M and a light one of mass m . In dimensionless units, the relative motion of these quantum particles is then governed by the stationary Schrödinger equation

$$\left[-\frac{1}{2} \Delta_{\vec{\xi}} - v_0 f(\xi) \right] \psi^{(2)}(\vec{\xi}) = \mathcal{E}^{(2)} \psi^{(2)}(\vec{\xi}) \quad (1)$$

for the wave function $\psi^{(2)}(\vec{\xi})$ and two-particle energy $\mathcal{E}^{(2)}$, where $\Delta_{\vec{\xi}}$ denotes the Laplace operator with respect to the relative coordinate $\vec{\xi}$. Here, we have assumed that the interaction of the two particles is described by an attractive potential $-v_0 f(\xi)$ of the magnitude $v_0 > 0$ and the shape $f(\xi)$ as a function of the relative distance $\xi \equiv |\vec{\xi}|$.

Next, we turn to the mass-imbalanced three-body system displayed in Fig. 1 and confined to (a) one or (b) two spatial dimensions. This system is governed by the dimensionless form of the stationary Schrödinger equation

$$\left[-\frac{\alpha_x}{2} \Delta_{\vec{x}} - \frac{\alpha_y}{2} \Delta_{\vec{y}} + V(\vec{x}, \vec{y}) \right] \psi = \mathcal{E} \psi \quad (2)$$

for the three-particle wave function $\psi = \psi(\vec{x}, \vec{y})$ corresponding to the three-particle energy \mathcal{E} , as introduced in more detail in Refs. [7, 8] for the one-dimensional case. Here $\Delta_{\vec{x}}$ and $\Delta_{\vec{y}}$ denote the Laplace operator with respect to the coordinate vectors \vec{x} and \vec{y} , respectively. The positive coefficients $\alpha_x = 2/(1+\alpha)$ and $\alpha_y = (1+2\alpha)/(2+2\alpha)$ are determined by the mass ratio $\alpha \equiv M/m$ of the heavy and light particle.

For the case of non-interacting heavy particles, the interaction term in Eq. (2)

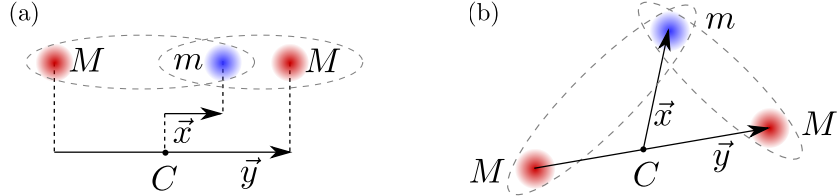


Figure 1: Three-body system consisting of two heavy particles of mass M and a light one of mass m confined to (a) one or (b) two spatial dimensions. We only allow for interactions between heavy and light particles, as indicated by the gray ellipses, and describe the system in terms of the Jacobi coordinates \vec{x} and \vec{y} , where C denotes the center-of-mass of the two heavy particles.

is described by the potential

$$V(\vec{x}, \vec{y}) = -v_0 f\left(\left|\vec{x} + \frac{1}{2}\vec{y}\right|\right) - v_0 f\left(\left|\vec{x} - \frac{1}{2}\vec{y}\right|\right), \quad (3)$$

where $-v_0 f(\xi)$ models the interaction potential between the light particle and each heavy one. Here $|\vec{x} \pm \vec{y}/2|$ is the respective relative distance in (a) one or (b) two spatial dimensions.

Our procedure to solve the three-body problem governed by Eq. (2) is as follows. First, we choose a particular binding energy $\mathcal{E}_0^{(2)}$ for the two-body system of the heavy and light particle. Then we determine the depth v_0 of the potential $-v_0 f(\xi)$ such that the two-body Schrödinger equation (1) has the ground state solution with energy $\mathcal{E}^{(2)} = \mathcal{E}_0^{(2)}$. Next, we solve the three-body Schrödinger equation (2) for this particular potential depth v_0 and select solutions with an energy smaller than the two-body threshold given by $\mathcal{E}_0^{(2)}$. In this way, we determine the wave functions $\psi(\vec{x}, \vec{y})$ and corresponding energies \mathcal{E} of three-body bound states associated with this particular two-body interaction.

For the demonstration of our approach, we consider in the present article an attractive potential of Gaussian shape with

$$f(\xi) = \exp(-\xi^2). \quad (4)$$

However, we emphasize that our approach is also valid for potentials that feature a different shape as a function of the relative coordinate ξ .

3. Discretization and tensor formulation

In this section, we briefly describe the discretization of the three-body Schrödinger equation by pseudo-spectral methods and, in particular, the Lagrange-mesh method [9]. In contrast to finite difference or finite element methods, pseudo-spectral methods lead to dense matrices for one-dimensional problems.

As a consequence, we obtain a faster convergence rate with respect to the number of grid points which is geometric on a finite domain and usually subgeometric on an infinite domain [10].

Since the three-body Hamiltonian is multi-dimensional, we aim to exploit its tensor structure when implementing the matrix-vector multiplication in an iterative eigenvalue solver. This drastically reduces the memory requirement for the operator when solving higher-dimensional eigenvalue problems.

3.1. Discretization

In the following, we apply a pseudo-spectral method to build a matrix representation of the Schrödinger equation (2) of the three-body problem. For this purpose, we consider Chebyshev polynomials as basis functions on a finite domain in each dimension. The corresponding grid points are then associated with the roots of the Chebyshev polynomials. Due to the structure of the three-body problem, we project these grid points to the infinite real domain via an algebraic map [10, 11].

After discretization, the Schrödinger equation (2) takes the form

$$H\vec{\psi} = \mathcal{E}\vec{\psi}, \quad (5)$$

which is a linear eigenvalue problem for the matrix H with eigenvalue \mathcal{E} and eigenvector $\vec{\psi}$.

For the one-dimensional three-body problem, the eigenvector

$$\vec{\psi}^{(1D)} \equiv \{\psi_{0,0}, \psi_{0,1}, \dots, \psi_{0,N_{y_1}-1}, \psi_{1,0}, \dots, \psi_{N_{x_1}-1, N_{y_1}-1}\}^T \quad (6)$$

corresponds to the wave function $\psi(\vec{x}, \vec{y}) = \psi^{(1D)}(x_1, y_1)$ in Eq. (2) evaluated at the grid points $(x_1^{(i)}, y_1^{(j)})$, yielding the entries $\psi_{i,j} = \psi^{(1D)}(x_1^{(i)}, y_1^{(j)})$ with $i = 0, 1, \dots, N_{x_1} - 1$ and $j = 0, 1, \dots, N_{y_1} - 1$. Here N_{x_1} and N_{y_1} denote the number of grid points in the respective direction.

Moreover, the matrix H in Eq. (5) takes the form

$$H^{(1D)} = -\frac{\alpha_x}{2} (D_{x_1 x_1} \otimes \mathbb{I}_{y_1}) - \frac{\alpha_y}{2} (\mathbb{I}_{x_1} \otimes D_{y_1 y_1}) + v_0(F_+ + F_-). \quad (7)$$

Here $D_{x_1 x_1}$ and $D_{y_1 y_1}$ are dense (generally non-symmetric) matrices with sizes $N_{x_1} \times N_{x_1}$ and $N_{y_1} \times N_{y_1}$ corresponding to the partial second derivatives $\partial^2 / \partial x_1^2$ and $\partial^2 / \partial y_1^2$ from the Laplace operators $\Delta_{\vec{x}}$ and $\Delta_{\vec{y}}$ in Eq. (2), respectively. Moreover, \mathbb{I}_{x_1} and \mathbb{I}_{y_1} denote the identity matrices of corresponding size. In addition, the diagonal matrices F_{\pm} result from evaluating the functions $f(|\vec{x} \pm \vec{y}/2|)$ determining the potential $V(\vec{x}, \vec{y})$, Eq. (3), at the grid points $x_1^{(i)}$ and $y_1^{(j)}$. More

details on the discretization procedure and the exact form of the matrices in Eq. (7) have been presented in Appendix B of Ref. [7].

Similarly, for the three-body problem in two dimension we perform a discretization of the wave function $\psi(\vec{x}, \vec{y}) = \psi^{(2D)}(x_1, x_2, y_1, y_2)$ with respect to the grid points $(x_1^{(i)}, x_2^{(j)}, y_1^{(k)}, y_2^{(l)})$. The matrix H in Eq. (5) then reads

$$H^{(2D)} = -\frac{\alpha_x}{2} [(\mathbf{D}_{x_1 x_1} + \mathbf{D}_{x_2 x_2}) \otimes \mathbb{I}_y] - \frac{\alpha_y}{2} [\mathbb{I}_x \otimes (\mathbf{D}_{y_1 y_1} + \mathbf{D}_{y_2 y_2})] + v_0 (\mathbf{F}_+ + \mathbf{F}_-), \quad (8)$$

where $\mathbf{D}_{x_1 x_1} = (D_{x_1 x_1} \otimes \mathbb{I}_{x_2})$, $\mathbf{D}_{x_2 x_2} = (\mathbb{I}_{x_1} \otimes D_{x_2 x_2})$, $\mathbb{I}_x = \mathbb{I}_{x_1} \otimes \mathbb{I}_{x_2}$, etc. Also here the diagonal matrices \mathbf{F}_\pm result from evaluating the function $f(|\vec{x} \pm \vec{y}/2|)$ in Eq. (3) at the grid points.

3.2. Operator application for the 1D case

When using an iterative method for solving the linear eigenvalue problem given by the discretized Schrödinger equation (5), only the effect of the linear operator on a given vector has to be implemented. Our 1D Hamiltonian $H^{(1D)}$, Eq. (7), can be abstractly written in the form

$$T_{V,a_1,a_2} = a_1 (C_1 \otimes \mathbb{I}_2) + a_2 (\mathbb{I}_1 \otimes C_2) + V \quad (9)$$

with, in this case, $C_1 = D_{x_1 x_1}$ and $C_2 = D_{y_1 y_1}$, and a sparse (in our case diagonal) matrix $V = v_0(F_+ + F_-)$. Note that we do not assume any structure for the potential operator V , in particular, it does not have to be of tensor structure $\mathbb{I}_1 \otimes A + B \otimes \mathbb{I}_2$ with matrices A, B . The application of the operator T_{V,a_1,a_2} , Eq. (9), to a vector w can be implemented efficiently by using dense matrix-matrix products. Let $C_1 \in \mathbb{R}^{N_1 \times N_1}$, $C_2 \in \mathbb{R}^{N_2 \times N_2}$, $w \in \mathbb{R}^{N_1 N_2}$. Let $W = \text{reshape}(w, N_2, N_1)$ denote the interpretation of w as an $N_2 \times N_1$ matrix. Then

$$T_{V,a_1,a_2} \cdot w = \text{reshape}(a_2 C_2 \cdot W + a_1 W \cdot C_1^T, N_1 N_2, 1) + V \cdot w, \quad (10)$$

where the reshape operation is used to interpret the resulting $N_2 \times N_1$ -matrix as a vector of length $N_1 N_2$. Note that reshape does not incur any data movement, it is just a re-interpretation of a vector as a matrix stored in column-major ordering, and vice versa.

Assuming that $N_{x_1} = N_{y_1} = n$, the storage requirement of the Hamiltonian operator in 1D is now only $\mathcal{O}(n^2)$ as compared to $\mathcal{O}(n^3)$ when storing it in a sparse matrix format. The performance of the $\mathcal{O}(n^3)$ arithmetic operations is limited by the floating point units of the hardware (compute bound). In general, an operation is compute bound if the arithmetic intensity I_c , defined as the ratio of required floating point operations (flops) and bytes of memory

transferred, is larger than the machine balance I_M , defined as the ratio of the peak floating point performance and the memory bandwidth of the hardware. For our matrix-matrix products, $I_c = \mathcal{O}(n)$ byte/flops, which is above the machine balance I_M on typical CPUs. For example, the Intel(R) Xeon(R) Gold 6152 CPU used for our 2D simulations in Section 5.2 achieves a memory bandwidth (pure load) of 60 GB/s and can perform about 1500 Gflop/s when running at its base frequency of 2.1 GHz, yielding $I_M \approx 25$ flops/byte. Applying the operator V to w is a memory-bound operation in general, because it requires only two flops per matrix entry loaded. Consequently, its cost is $\mathcal{O}(n^2)$ memory transfers.

If $H^{(1D)}$ is represented as a sparse matrix, then loading and applying the operator T_{V,a_1,a_2} , Eq. (10), would cost $\mathcal{O}(n^3)$ memory transfers and still $\mathcal{O}(n^3)$ flops. The operation is then memory bound as $I_c = \mathcal{O}(1)$. So the high values of I_M in modern HPC hardware like CPUs and GPUs can lead to a speed-up of about a factor 100 when going from the sparse matrix representation to the tensor operations that we propose in this article. As an example, for the processor mentioned above and $I_c = 1$, we would achieve a performance 200 times below the peak floating point performance for double precision data.

3.3. Operator application for the 2D case

For the 2D problem, both the operator $H^{(2D)}$, Eq. (8), and its components $\mathbf{D}_{xx} = \mathbf{D}_{x_1x_1} + \mathbf{D}_{x_2x_2}$, $\mathbf{D}_{yy} = \mathbf{D}_{y_1y_1} + \mathbf{D}_{y_2y_2}$ are of the form Eq. (9) with particular choices of a_1 , a_2 , and V . Thus, we can now apply Eq. (10) in a nested way. Let $W = \text{reshape}(w, N_{y_1} N_{y_2}, N_{x_1} N_{x_2})$ and $N = N_{x_1} N_{x_2} N_{y_1} N_{y_2}$. Then we arrive at

$$H^{(2D)} \cdot w = \text{reshape} \left(-\frac{\alpha_y}{2} \mathbf{D}_{yy} \cdot W - \frac{\alpha_x}{2} W \cdot \mathbf{D}_{xx}^T, N, 1 \right) + V \cdot w. \quad (11)$$

If we assume that $N_{x_1} = N_{x_2} = N_{y_1} = N_{y_2} = n$, then loading the operator still requires $\mathcal{O}(n^2)$ memory transfers. However, the vector w now actually represents 4D tensors and has a storage requirement of $\mathcal{O}(n^4)$. Hence, the total amount of memory transferred is $\mathcal{O}(n^4)$. For each of the n^2 columns of W , $\mathcal{O}(n^3)$ flops are performed, amounting to $\mathcal{O}(n^5)$ in total. The computational intensity is therefore still $\mathcal{O}(n)$, so the operation is compute bound as before. In practice, we implement the term $W \mathbf{D}_{xx}^T$ as $(\mathbf{D}_{xx} W^T)^T$, so that n^4 vector elements have to be read and written twice in each operator application due to the transpose operations. This overhead can be avoided by using an optimized implementation of a tensor contraction, such as GETT [12].

4. Jacobi-Davidson and preconditioning

In this section we briefly introduce the Jacobi-Davidson QR (JDQR) method [13]. Compared to the Arnoldi-type iteration (Krylov-Schur) implemented in Matlab's `eigs` command, JDQR offers some flexibility when solving the so-called correction equation. We use this flexibility to improve the convergence dramatically by introducing a preconditioned iteration for the correction equation, exploiting again the tensor structure of the matrices.

4.1. The Jacobi-Davidson QR Method

We use a Matlab implementation of the JDQR method [13] that is suitable for computing a few exterior eigenvalues of a non-Hermitian matrix. The algorithm computes a partial QR decomposition of a matrix A by applying a Newton process to the system of equations

$$\begin{cases} AQ - QR &= 0, \\ -\frac{1}{2}Q^T Q + \frac{1}{2}\mathbb{I} &= 0. \end{cases} \quad (12)$$

The Newton updates are used to extend the search space spanned by Q and the standard Ritz pairs are used for approximating eigenpairs of the matrix A . Whenever the basis spanning the search space reaches a maximum size m_{max} , it is compressed into m_{min} vectors by (implicitly) applying a truncated Singular Value Decomposition (SVD) to retain only the most relevant directions.

The Newton process requires solving the correction equation

$$(\mathbb{I} - \tilde{Q}\tilde{Q}^T)(A - \theta\mathbb{I})(\mathbb{I} - \tilde{Q}\tilde{Q}^T)\Delta q = -(Aq - q\theta) \quad (13)$$

for the new basis vector Δq in every outer iteration i . Here \tilde{Q} contains the approximation $q \approx Q_i$ for the current eigenvector, and any previously converged ('locked') eigenvectors, $\theta \approx R_{ii}$ denotes the current approximate eigenvalue.

The deflation operator $\mathbb{I} - \tilde{Q}\tilde{Q}^T$ improves the conditioning of the shifted matrix $A - \theta\mathbb{I}$. We will employ a Generalized Minimal Residual (GMRES) method for solving Eq. (13) with additional acceleration by preconditioning, as discussed in the next section. Further details on how the preconditioner is combined with the projections can be found in [14].

4.2. Preconditioning

In order to improve the convergence of the GMRES correction solver, we introduce a shifted version of the Hamiltonian that ignores the potential V . We neglect V in the preconditioner so that we can exploit the tensor product

structure of the differential operator even if V does not have tensor structure, as discussed above.

In the 1D case, for small values of the potential depth v_0 , the matrix $H^{(1D)}$, Eq. (7), can be approximated by an operator of the form $T_{0,1,1}$ presented in Eq. (10), where $C_1 = -\frac{\alpha_y}{2}D_{y_1y_1}$, $C_2 = -\frac{\alpha_x}{2}D_{x_1x_1}$. For some scalar σ , linear systems with $T_{0,1,1} - \sigma\mathbb{I}$ and some right-hand side b , respectively $B = \text{reshape}(b, N_{y_1}, N_{x_1})$, can be solved for w with the help of the Sylvester equation

$$(C_1 - \sigma_1\mathbb{I}_1)W + W(C_2 - \sigma_2\mathbb{I}_2)^T = B \quad (14)$$

where $\sigma = \sigma_1 + \sigma_2$. For our system, the shift $\sigma_{1,2} = -\alpha_{y,x}\mathcal{E}_0^{(2)}/|\alpha_x + \alpha_y|$ is a good choice. In this case the preconditioner approximates the shift-invert operator near the value $-\mathcal{E}_0^{(2)}$ of the two-body binding energy, which is close to the desired eigenvalues.

Bartels and Stewart [15] have introduced a direct method for solving the Sylvester equation (14). It requires a Schur decomposition of the shifted matrices $C_{1,2} - \sigma_{1,2}\mathbb{I}$, and subsequently a combination of two dense matrix-matrix products and a special forward/backward substitution with the Schur factors. Since the matrices involved remain the same throughout the JDQR process, the Schur factorization has to be performed only once. Applying our preconditioner again has a computational cost of $\mathcal{O}(n^3)$ and requires $\mathcal{O}(n^2)$ data transfers, so that the performance characteristics of the overall algorithm are unchanged.

Unfortunately, we cannot straightforwardly extend our preconditioner, which is a direct solver for a shifted operator, to the 2D case. Indeed, the Schur decomposition of the operators D_{xx} and D_{yy} cannot be simply represented as a sum of Kronecker product terms. Instead one could use an iterative procedure to approximate the effect of the shift-invert operator in 2D, but we do not investigate such techniques here. Numerical results for the 2D case without preconditioning are shown in Section 5.2.

5. Numerical and performance results

In this section, we present the results for our numerical study of the quantum mechanical three-body problem in one and two spatial dimensions. We investigate the convergence of the three-body energies as a function of the number of grid points. Moreover, we compare the performance of three iterative eigenvalue solvers: Krylov-Schur and Jacobi-Davidson QR with respectively without preconditioning.

5.1. Results for the three-body problem in 1D

In order to compute the bound states of the three-body problem in 1D, we solve the discretized Schrödinger equation (5). To increase the accuracy at a given grid resolution, we apply the parity selection rule to the problem, in order to reduce the problem size for a given accuracy by a factor of 2^2 . This technique exploits the symmetry properties of the basis functions used for discretization by following the procedure outlined in Ref. [16]. In practice, this means that bosonic and fermionic bound states have to be computed separately. These particular states are characterized by even respectively odd wave functions with regard to the transformation $\vec{y} \rightarrow -\vec{y}$ corresponding to the exchange of the two heavy particles shown in Fig. 1.

First, we determine the potential depth v_0 such that it corresponds to a particular two-body binding energy $\mathcal{E}_0^{(2)}$. For this purpose, we choose a particular value of the two-body binding energy $\mathcal{E}^{(2)} = \mathcal{E}_0^{(2)}$ in the discretized version of the Schrödinger equation (1) in 1D and solve the generalized eigenvalue problem for the lowest eigenvalue v_0 . For the two-body binding energies $\mathcal{E}_0^{(2)} = 10^{-1}, 10^{-2}$, and 10^{-3} , the lowest potential depths v_0 are listed in Table 1. These parameters are then used for solving the discretized three-body problem in 1D, Eq. (5), with the Hamiltonian matrix given by Eq. (7). For bosonic and fermionic heavy particles with a mass ratio $\alpha = M/m = 20$ between heavy and light particle, we include the resulting ratios $\mathcal{E}/\mathcal{E}_0^{(2)}$ of three-body and two-body binding energy in Table 1. Our results coincide with the ones presented in Ref. [7] and as $\mathcal{E}_0^{(2)} \rightarrow 0$ they approach the universal values shown in Table 1 of Ref. [8].

Table 1: Computed ratio $\mathcal{E}/\mathcal{E}_0^{(2)}$ of three-body and two-body binding energy in one dimension for the case of two heavy bosons or fermions as obtained by solving the discretized Schrödinger equation (5). The calculations are performed for a mass ratio $\alpha = 20$ of heavy and light particles, interacting via a Gaussian shaped potential $f(\xi)$, Eq. (4). Here the potential depth v_0 has been chosen such that it corresponds to a particular two-body binding energy $\mathcal{E}_0^{(2)}$.

$\mathcal{E}_0^{(2)}$	v_0 in 1D	eigenvalues: bosonic	fermionic
10^{-1}	0.344595351	-2.47603458	-1.82589653
		-1.41279329	-1.18259157
		-1.06093864	-1.02845702
10^{-2}	0.088873721	-2.66187629	-1.68983501
		-1.33267928	-1.13394640
		-1.03860624	-1.00258200
10^{-3}	0.026134366	-2.71516265	-1.65622442
		-1.32865305	-1.12520220
		-1.03745282	-1.00045248

In order to test the convergence of our results, we use a sequence of grid sizes N_{x_1} and always choose $N_{y_1} = N_{x_1}/2$. The results in Fig. 2 confirm the excellent

convergence properties of the discretization: The relative spatial discretization error, estimated by the relative difference of the computed eigenvalues on successive grids, quickly reaches the tolerance of 10^{-12} set in the solver for the computation of each eigenpair.

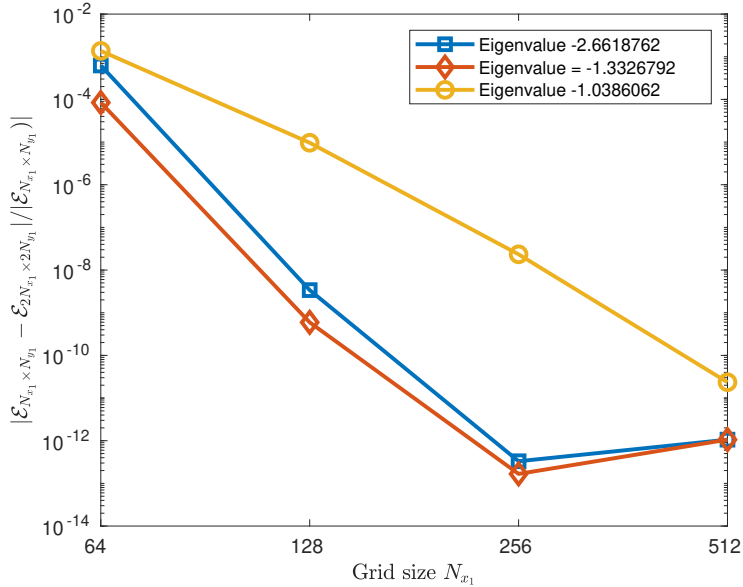


Figure 2: Relative spectral discretization error $|\mathcal{E}(N_{x_1} \times N_{y_1}) - \mathcal{E}(2N_{x_1} \times 2N_{y_1})| / |\mathcal{E}(N_{x_1} \times N_{y_1})|$ for the three bosonic eigenvalues. The tolerance in the eigenvalue solver has been set to 10^{-12} .

Next, we compare the convergence behavior and running time of three methods, namely the Krylov-Schur (KS) and JDQR method, without (no-prec) and with (prec) preconditioning as described in Section 4.2. In each case we exploit the tensor structure of the problem when applying the linear operator.

For different two-body binding energies $\mathcal{E}_0^{(2)}$, we present in Table 2 a comparison of the number of iterations and matrix-vector multiplications (MVM) necessary for computing the three lowest 1D three-body bound energies shown in Table 1 with the KS and no-prec/prec-JDQR methods. All the solvers have been set to the same tolerance $\text{tol} = 10^{-12}$. The results shown here are for the bosonic heavy particles, but the behavior is very similar for fermionic ones.

Compared to KS, the no-prec-JDQR substantially reduces the number of matrix-vector multiplications, each of which in fact is an operator application of the discretized Hamiltonian, as described in Section 3.2. This is explained by the superior convergence rate of the inexact Newton process within JDQR over the Krylov subspace iteration. The prec-JDQR achieves an even more drastic reduction of the number of iterations and MVMs. This is due to the fact that the

correction equation can now be solved to sufficient accuracy in order to achieve locally quadratic convergence of the Newton process. In addition to the MVM, this method requires a similar number of preconditioner applications, which have a similar cost as discussed in Section 4.2. As a consequence of the fast convergence, the running time required to find the eigenvalues is significantly reduced, as shown in Fig. 3. In this work a Matlab implementation of our methods was used and the Matlab-command `eigs` implemented the KS method.

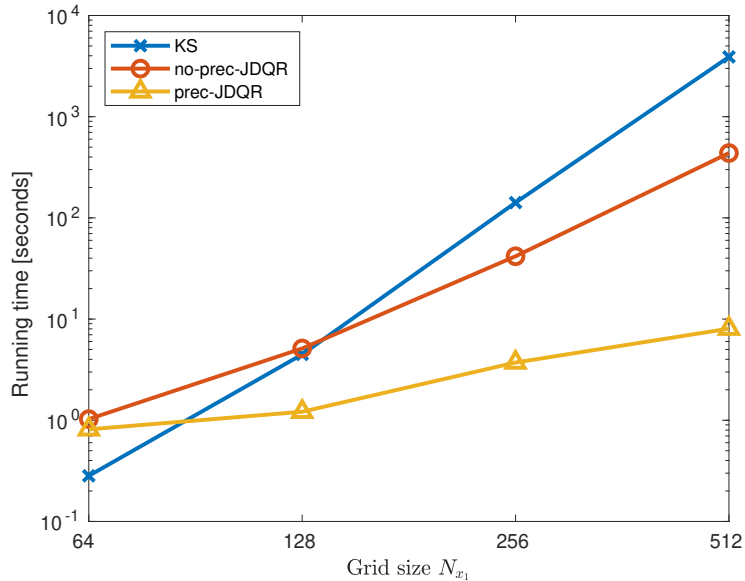


Figure 3: Comparison of running time for computing the three bosonic bound states for the case of $\mathcal{E}_0^{(2)} = 10^{-2}$ with the KS, no-prec-JDQR, and prec-JDQR methods.

5.2. Preliminary results for the three-body problem in 2D

The aim of this section is not to provide conclusive results for the three-body problem in 2D. Instead, we highlight the viability of our approach to study this system. We have developed a multi-threaded C++ implementation of the model and techniques described to evaluate the feasibility of simulations in 2D. The dense linear algebra operations are provided by Intel MKL (version 2020.4.304) and the JDQR method by phist [14], version 1.9.6. The backend used within phist is the Trilinos library Tpetra [17], version 13.0.1.

Our discretization scheme uses $N_{x_1} = N_{x_2} = N_x$ points in the x_1 and x_2 -directions, and $N_{y_1} = N_{y_2} = N_y$ points in the y_1 and y_2 -direction, leading to a total problem size of $N = N_x^2 N_y^2$, where we choose again $N_y = N_x/2$. The numerical simulations are run on an Intel Xeon server with 20 cores and 128 GB of RAM. For the $(128 \times 64)^2$ grid, computing ten digits of the lowest eigenvalue took about one hour at $\mathcal{E}_0^{(2)} = 10^{-2}$.

Table 2: Comparison of the number of iterations and matrix-vector multiplications $\#MVM$ necessary to compute the lowest three eigenpairs using Krylov-Schur (KS), Jacobi-Davidson, without preconditioner (no-prec-JDQR) and with preconditioner (prec-JDQR), respectively.

$\mathcal{E}_0^{(2)}$	N_x	N_y	KS	$\#MVM$	no-prec-JDQR	$\#MVM$	prec-JDQR	$\#MVM$
10^{-1}	64	32	134	2082	56	1182	24	253
	128	64	1086	16491	132	2920	28	258
	256	128	5211	80523	299	6782	28	261
	512	256	11324	172018	679	15526	37	506
	1024	512					42	540
10^{-2}	64	32	88	1390	46	932	25	206
	128	64	720	10999	92	2004	28	292
	256	128	6072	91977	212	4765	29	337
	512	256	23546	357133	554	12648	30	402
	1024	512					39	502
10^{-3}	64	32	34	560	40	792	23	163
	128	64	170	2728	74	1596	25	202
	256	128	2200	33815	148	3303	28	235
	512	256	13599	207748	367	8342	28	265
	1024	512					34	271

We consider the mass ratio $\alpha = 1$ and the two-body binding energy $\mathcal{E}_0^{(2)} = 10^{-1}$, respectively 10^{-2} , for which we have calculated the corresponding value v_0 for the Gaussian interaction potential as shown in Table 3. For this situation, we expect only one bound state as $\mathcal{E}_0^{(2)} \rightarrow 0$, with an energy of approximately $2.39 \mathcal{E}_0^{(2)}$ [18] or $2.36 \mathcal{E}_0^{(2)}$ [19]. Our numerical results are summarized in Table 3. The computed values of the three-body binding energy, relative to $\mathcal{E}_0^{(2)}$, indicate convergence for the value $\mathcal{E}_0^{(2)} = 10^{-1}$ to at least eight digits. For the smaller value $\mathcal{E}_0^{(2)} = 10^{-2}$, the lowest eigenvalue is approaching the expected universal limit value of approximately -2.4 . Decreasing $\mathcal{E}_0^{(2)}$ to get closer to this value in turn requires a larger computational domain and thus more grid points in order to accommodate the bound states.

Table 3: Preliminary results for the lowest eigenvalue $\mathcal{E}/\mathcal{E}_0^{(2)}$ of the three-body problem in 2D with mass ratio $\alpha = 1$ for successively refined grids.

$\mathcal{E}_0^{(2)}$	v_0 in 2D	$(32 \times 16)^2$	$(64 \times 32)^2$	$(128 \times 64)^2$	$(144 \times 72)^2$	$(160 \times 80)^2$
10^{-1}	0.947343916	-1.9012589	-2.1984679	-2.1999578	-2.1999578	-2.1999578
10^{-2}	0.482727283	-	-1.9337722	-2.2878081	-2.3021863	-2.3081557

We consider two improvements of our current implementation to enable such simulations: First, it may be possible to exploit the parity rule (as in the 1D case) to reduce the problem size for a given accuracy by a factor of 2^4 . The details have to be clarified, though. Second, hybrid shared/distributed memory

parallelization should allow us to increase the grid size by a factor four in each direction (problem size by a factor 256) on a cluster with a few hundred nodes. In order to go to very small binding energies (large grid sizes), an alternative may be to enforce a low-rank structure on the occurring vectors in order to reduce the memory requirement for vectors in a similar way that we have used to reduce the memory requirement for the operator in this paper.

6. Conclusion and outlook

In this article, we have considered a quantum system of two heavy particles interacting with a light one in both 1D and 2D. Pseudo-spectral methods and (rational) Chebyshev polynomials have been applied to create a fast converging discretization scheme for the Hamiltonian. Moreover, we have presented a novel method to exploit the tensor structure of the discretized Hamiltonian in iterative eigensolvers. The improved hardware efficiency of our tensor-based implementation is expected to deliver a speed-up of about a factor 100 when compared to the sparse matrix representation used in previous studies of the three-body problem.

Based on the direct solution of a Sylvester equation, we have developed an effective preconditioning strategy for the 1D problem. This preconditioner is then applied to accelerate a Jacobi-Davidson QR iterative eigensolver. Our numerical simulations confirm the convergence rate of the discretization and demonstrate an improvement of orders of magnitude in the time-to-solution for the preconditioned Jacobi-Davidson method over previously used Krylov methods. Combined with the additional factor of 100 resulting from the increased hardware efficiency of our implementation, this will allow studying the three-body problem more thoroughly than before.

To enable extensive numerical simulations of the 2D problem in the future, we will follow the paths identified above, namely exploiting symmetry, hybrid parallelization and low-rank approximation. As an outlook, the three-body problem in 1D and 2D can also be investigated with a focus on the computation of bound and resonant states embedded in the continuous spectrum. The methods developed in the present article will strongly support this endeavor.

References

- [1] V. Efimov. Energy levels arising from resonant two-body forces in a three-body system. *Phys. Lett. B*, 33:563, 1970.
- [2] V. Efimov. Energy levels of three resonantly interacting particles. *Nucl. Phys. A*, 210:157, 1973.

- [3] Y. Nishida, S. Moro, and D. T. Son. Super Efimov Effect of Resonantly Interacting Fermions in Two Dimensions. *Phys. Rev. Lett.*, 110:235301, 2013.
- [4] S. Moroz and Y. Nishida. Super Efimov effect for mass-imbalanced systems. *Phys. Rev. A*, 90:063631, 2014.
- [5] D.K. Gridnev. Three resonating fermions in flatland: proof of the super Efimov effect and the exact discrete spectrum asymptotics. *J. Phys. A*, 47:505204, 2014.
- [6] A. Volosniev, D. Fedorov, A. Jensen, and N. Zinner. Borromean ground state of fermions in two dimensions. *J. Phys. B*, 47:185302, 2014.
- [7] L. Happ, M. Zimmermann, S.I. Betelu, W.P. Schleich, and M.A. Efremov. Universality in a one-dimensional three-body system. *Phys. Rev. A*, 100:012709, 2019.
- [8] L. Happ, M. Zimmermann, and M.A. Efremov. Universality of excited three-body bound states in one dimension. *J. Phys. B.*, 2021. (in press).
- [9] D. Baye. The Lagrange-mesh method. *Phys. Rep.*, 565:1–107, 2015.
- [10] J.P. Boyd. *Chebyshev and Fourier Spectral Methods*. Dover, New York, 2000.
- [11] J.P. Boyd. Spectral Methods Using Rational Basis Functions on an Infinite Interval. *J. Comput. Phys.*, 69:112, 1987.
- [12] P. Springer and P. Bientinesi. Design of a high-performance GEMM-like tensor–tensor multiplication. *ACM Transactions on Mathematical Software*, 44, 2018.
- [13] R. Fokkema, G. Sleijpen, and H. Van der Vorst. Jacobi-Davidson style QR and QZ algorithms for reduction of matrix pencils. *SIAM J. Sci. Comp.*, 20:94–125, 1998.
- [14] J. Thies, M. Röhrig-Zöllner, N. Overmars, A. Basermann, D. Ernst, G. Hager, and G. Wellein. PHIST: a Pipelined, Hybrid-parallel Iterative Solver Toolkit. *ACM Trans. Math. Software*, 46, 2020.
- [15] R. Bartels and G. Stewart. Solutions of the matrix $AX+BC = C$. *Communications of the ACM*, 15:820–826, 1972.
- [16] L.N. Trefethen. *Spectral methods in MATLAB*. SIAM, Philadelphia, 2000.

- [17] M.A. Heroux, R.A. Bartlett, V.E. Howle, R.J. Hoekstra, J.J. Hu, T.G. Kolda, R.B. Lehoucq, K.R. Long, R.P. Pawlowski, E.T. Phipps, A.G. Salinger, H.K. Thornquist, R.S. Tuminaroand, J.M. Willenbring, A. Williams, and K. Stanley. An overview of trilinos. *ACM Trans. Math. Softw.* 31, 3, pages 297–423, 2005.
- [18] I.V. Brodsky, M.Y. Kagan, A.V. Klaptsov, R. Combescot, and X. Leyronas. Exact diagrammatic approach for dimer-dimer scattering and bound states of three and four resonantly interacting particles. *Phys. Rev. A*, 73:032724, 2006.
- [19] L. Pricoupenko and P. Pedri. Universal (1+2)-body bound states in planar atomic waveguides. *Phys. Rev. A*, 82:033625, 2010.